A DFT study of diesel exhaust NO_x reduction over rare earth CeO_2 catalyst

He Huang [1,*], *Xiao Zhang*[2]

[1] School of Traffic Engineering, Nanjing Institute of Industry Technology, Nanjing 210046, China

[2] Zhenjiang Campus, Army Military Transportation University of PLA, Zhenjiang 212000, China

Abstract. Adsorption of NO on the CeO2(110) surface was investigated using RPBE approach of GGA within the framework of density functional theory (DFT) combined with periodic slab model. Two molecular orientations, N-end and O-end, over various adsorption sites, top, hollow, bridge and O site of CeO2(110) sur-face have been considered. Two molecular orientations under different coverage of CeO2(110) surface also have been considered. The optimized results indicate that the N-end adsorption models are more stable than the O-end ones. So N-end adsorption was more favourable than O-end. NO adsorption on a clean CeO2(110) surface was physisorption, while chemical adsorption occurred in the present of surface oxygen vacancy. Adsorption is stable when coverage was set to 0.25 monolayer. Researched on density of states of free NO molecule and adsorbed NO molecule, the results show that there is an interaction between NO molecule and the substrate . The population analysis indicates that the charges transfer from Ce atoms to NO molecule. The charges transfer of O-end is more than N-end.

Cerium dioxide (CeO_2) is one of the most suitable three-way catalysts (TWCs) for automobile exhaust emission system[1]. It can simultaneously convers hydrocarbons (HCs), CO and NO_x from the exhaust into H_2O, CO_2 and N_2. CeO_2 functions as oxygen buffer due to its great capacity of oxygen storage/release[2-3]. The oxygen vacancy in CeO_2 enables fast oxygen storage when exhaust oxygen concentration is high, and opportune oxygen release when the concentration is low[4-5]. The key reactions for exhaust emission control are CO oxidation and NO_x reduction, and adsorption is the initial step for the reactions. In previous research, periodic density functional theory was implemented to study adsorption pattern of CO on CeO_2(110) and CeO_2(111) surfaces, which indicated the oxidation of CO was due to the lattice oxygen on CeO_2 surface.

There have been many studies about NO adsorption on CeO_2 surface. Ozeki et al. [6]found that high adsorption capacity of CeO_2 to NO ((4.9 molecules /nm^2) could be achieved under 303K. Nearly 40% NO chemically bind to CeO_2 as NO_2^-. Based on IR frequency analysis, it was speculated that Ce^{4+} converted to Ce^{3+} due to NO. Daturi et al. [7] analyzed infrared absorption spectra and mass spectrometry and proved that total oxygen exchange of CeO_2 was strongly correlated with NO activity and oxygen vacancy

* Corresponding author: 394807515@qq.com

concentration on CeO_2 surface. Ceria based catalysts have sufficient oxygen vacancy to accelerate NO decomposition. However, due to limitation of methods, it is unfeasible to reveal the site, configuration, energy and electronic structure of NO adsorption. Recently, designing new materials from atomic and molecular level has been widely used. Combined with experimental methods, it can greatly reduce dependency on instruments and chemical reagents and theoretically study underlying mechanisms of catalytic reactions. Therefore, it is a suitable ideology to find selective, active and anti-toxic catalyzer. In this paper, the interaction between NO and CeO_2 was discussed by theoretical calculation.

The NO adsorption pattern on CeO_2(110) surface was systemically studied under density functional theory framework[8-13]. Firstly, models of NO adsorption by N terminal and O terminal on various adsorption sites on CeO_2(110) surface were calculated. Secondly, stability and energy of adsorption sites of NO on CeO_2(110) surface with oxygen vacancy under different coverage were investigated and charge transformation was revealed by state density and layout analysis.

1 Model and Calculation

The Pure CeO_2 is cubic fluorite crystal with face-centered cubic atomic arrangement in unit cell. Each Ce atom is surrounded by eight oxygen atoms, with space group of Fm3m and lattice parameters of a=b=c=5.411Å , α=β=γ=90°[14]. The DFT calculation suggests CeO_2(110) surface has the lowest formation energy of oxygen vacancy to generate O_v, compared to CeO_2(100) and CeO_2(111) [15-16]. Therefore, it can provide more surface reactive oxygen species highly active in catalytic reactions[17]. In this research, CeO_2(110)-2×2 and CeO_2(110)-3×3 supercells were chosen for NO adsorption by N terminal and O terminal. Figure 1. Shows the models of CeO_2(110)-2×2 and CeO_2(110)-3×3 supercells.

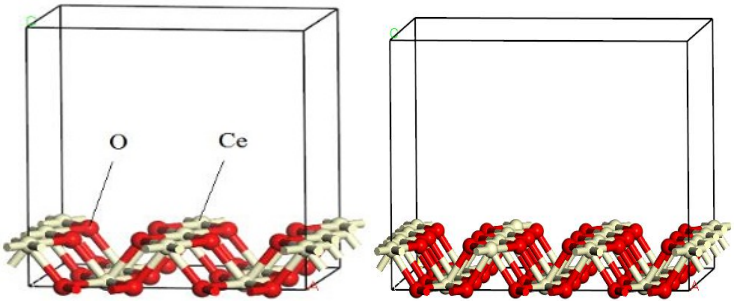

Fig.1. CeO_2(110)-2×2 and CeO_2(110)-3×3 supercell models.

The NO adsorption on CeO_2(110) surface was simulated by combined method of periodic slab model and GGA-RPBE of density functional theory. All calculation was carried out by $Dmol^3$ software kit[18-21]. For the calculation of geometry structure optimization and transition state, density functional theory has been proved to be a reliable tool[22]. Core electrons of CeO_2 atom was substituted by effective core potential (ECP) during calculation. The wave functions were expanded by double number polarization function (DNP). All electron basis set was implemented for N and O atoms. Cutoff energy was set as 380eV. Brillouin zone was sampled at k point with Monkhorst-Pack method[23]. The set of accuracy in energy calculation and structure optimization was as following: (1) Self-consistent field energy convergency was 1.0×10^{-4}eV (2) Maximum force was $0.2 eV\cdot nm^{-1}$. Converging energy from optimization was less than 1.0×10^{-3}eV. Through geometric optimization, bond length of N-O in free NO molecule was 1.169 Å, which was

similar to the result from experiments, 1.151Å[24]. 10 Å vacuum was reserved between two layers to erase potential interactions.

Formation energy of oxygen vacancy on CeO_2(110) surface was represented by:

$$E_V = E_{VCeO_2} + 1/2E_{O_2} - E_{CeO_2} \quad (1)$$

Where E_{VCeO2} was the energy of single oxygen vacancy on CeO_2(110) surface, E_{O2} was the energy of gas oxygen molecule, and E_{CeO2} was the surface energy of clean CeO_2.

The adsorption energy on clean CeO_2(110) surface was calculated as the change of total energy of all substances during the adsorption:

$$E_{ads} = E_{NO} + E_{substrate} - E_{(NO\ +substrate)} \quad (2)$$

Where E_{ads} was adsorption energy, E_{NO} was energy of NO before adsorption, $E_{substrate}$ was energy of substrate before adsorption. $E_{(NO+substrate)}$ was the energy of the whole system after adsorption. Minus value of E_{ads} indicated NO adsorption release heat, vice versa.

The adsorption energy on CeO_2(110) surface with oxygen vacancy was defined as:

$$E_{ads} = -(E_{NO\ /\ VCeO_2} - E_{NO} - E_{VCeO_2}) \quad (3)$$

Where E_{NO}/$VCeO_2$was the energy of NO and CeO_2 surface interaction system.

2 Results and discussion

2.1 The calculation of NO molecule

Firstly, the bond length and binding energy of NO molecule were calculated by different methods to verify the reliability of the method selected in this study. The results are shown in table 1. GGA-ROBE method generated closest results to experimental results. So this method was implemented in following steps.

Table 1. The bond length and binding energy of free NO molecule.

Method	R_{N-O} (Å)	BE (kJ/mol)
LDA-PWC	1.154	819.0
LDA-VWN	1.154	818.6
GGA-PW91	1.163	726.5
GGA-BP	1.165	705.7
GGA-PBE	1.164	727.1
GGA-BLYP	1.169	698.0
GGA-VWN-BP	1.169	698.0
GGA-RPBE	1.169	687.4
Exp	1.151	627.2[25]

2.2 The NO adsorption on clean CeO_2(110) surface and the surface with oxygen vacancy

2.2.1 The comparison of NO adsorption at various sites on CeO2(110) surface

In order to investigate the adsorption mode of NO on the surface of CeO_2(110), the geometric configuration parameters and adsorption energy of NO on the surface of CeO_2(110) with oxygen holes and clean were calculated. According to the projection position of center of NO on CeO_2(110) surface, four adsorption sites were considered, including Top site, Hollow site, Bridge site and O site. Figure 2 illustrates the four sites.

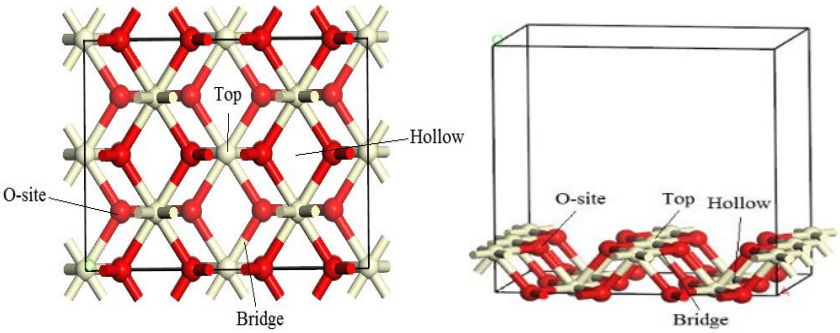

Fig.2. The slab model of CeO_2(110)-2×2(top and side views).

Table 2 indicates the adsorption energy under coverage of 0.25mL. On clean CeO_2(110) surface, the adsorption energy was less than 40kJ/mol and the adsorption was physical. N terminal adsorption was more stable than O terminal at each site. The energy of adsorption by N terminal was O **>** top **>** hollow **>** bridge. The energy was highest with N terminal at O site but only reached to 39.6 kJ/mol. The distance between N and O atoms was 2.55 Å. These results were consistent with the results from Yang et al[26], which suggests minimum NO adsorption occurred on CeO_2(110) surface with complete stoichiometric ratio. The increasing N-O bond length by adsorption suggests the adsorption weakened the NO bond, which is beneficial to further decomposition of NO. In this case, O terminal adsorption was more effective than N terminal adsorption.

Table 2. The predicted geometrical parameter and adsorption energies for NO on stoichiometry CeO_2(110) surface.

Adsorption site	Top site		Hollow site		Bridge site		O site	
	N	O	N	O	N	O	N	O
R_{N-O}(Å)	1.188	1.191	1.186	1.203	1.203	1.204	1.199	1.209
Eads/(kJ/mol)	17.4	8.55	15.3	6.2	13.3	4.8	39.6	17.66

2.2.2 NO adsorption on O_v/CeO_2(110) surface

Based on the above analysis, NO has the strongest adsorption at the n-terminal at the oxygen level, so we discuss the n-terminal adsorption at the oxygen level on the surface of O_v/CeO_2(110). Figure 3(a) is the structure of oxygen vacancy on CeO_2(110) surface. By calculation, the formation energy of oxygen vacancy was 180.4kJ/mol which was similar to the result from references[27]. Figure 3(b) was NO adsorption configuration on oxygen vacancy. After adsorption, NO bond length was 1.149Å, shorter than the bond length in free NO molecule. The oxygen significantly increased adsorption energy which were

135.1kJ/mol with N terminal and 80.1kJ/mol with O terminal. Additionally, there was certain interaction between NO and surface of oxygen vacancy. Therefore, NO adsorption will be more effective with N terminal on CeO_2(110) surface with oxygen vacancy.

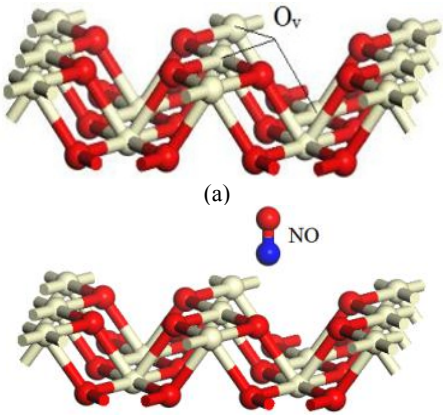

Fig.3. Optimized structures of surface oxygen vacancy (a) and NO adsorbed on the oxygen vacancy(b) O_v:oxygen vacancy;bond length in Å.

2.3 The active of NO adsorption on O_v/CeO_2(110) under different coverage

Geometric optimization was implemented to configuration under coverage of 0.25, 0.33, 0.50, 0.67mL and 1.00mL. Table 3 shows the results. The coverage was defined as ratio of number of adsorbed NO molecules and number of Ce atoms on the surface. For instance, when one NO adsorbed by CeO_2(110)-2×2 surface, the coverage was 0.25mL. From table 3, adsorption energy decreased with increasing coverage. However, the energy increased when coverage was 1.00mL. The reason was that due to decreasing distance between NO molecules the interaction of NO enhanced with increasing coverage. The decrease of systemic energy after adsorption caused increasing adsorption energy. The calculation of bond length suggested that the NO bond length increased after adsorption and reached highest under coverage of 0.25mL, which was most suitable for further reaction of NO.

Table 3. The predicted geometrical parameter and adsorption energies for NO over O_v/CeO_2(110) surface.

Coverage(mL)	0.25	0.33	0.50	0.67	1.00
$R_{N\text{-}O}$(Å)	1.199	1.196	1.187	1.185	1.182
E_{ads}/(kJ/mol)	135.1	129.3	107.5	106.8	115.2

To deeply understand the mechanisms of NO adsorption on O_v/CeO_2(110), state density was calculated before and after adsorption. The results are shown in Table 4. There was a peek of state density of free NO at Femi. Compared to Figure 4(a), there was obvious changes of state density of free NO in Figure 4(b)-(f), which suggested that NO interacted with substrate during adsorption and energy band shifted to low energy level. Based on these results, it was speculated that the formation of adsorption bond was caused by the interaction between d orbit in Ce atom and inverse π orbit in NO molecule. Since d orbit with full electrons while inverse π orbit contains electron vacancy, the electron transferred from d orbit to inverse π orbit, causing elongation of N-O bond.

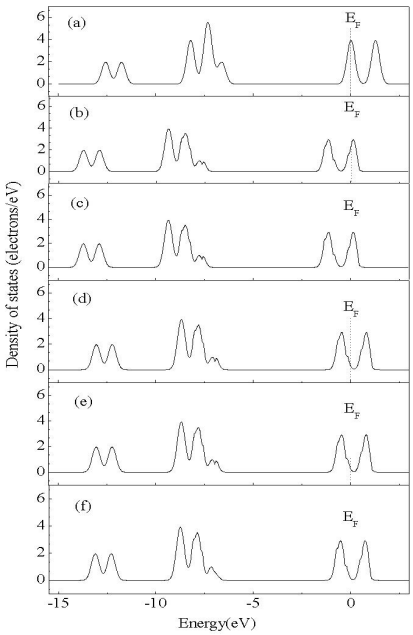

Fig.4. The density of states (DOS) of free NO molecule and adsorbed NO molecule under different coverages.
(a) Free NO, (b) 0.25 ML, (c) 0.33 ML,
(d) 0.50 ML, (e) 0.67 ML, (f) 1.00 ML

2.4 NO molecular layout analysis

The NO molecular layout under coverage of 0.25mL was further analyzed. Table 4 shows the Mulliken charge density of N and O atoms when NO was adsorbed on $O_v/CeO_2(110)$ with N and O terminal. The charges of N and O atoms both changed, and O terminal shifted more than N terminal. It was because O atom contained greater electronegativity and more tended to attract electrons. Negative charge appeared on NO after adsorption which indicated electrons transferred form Ce to NO. This was consistent with the results of state density analysis. Based on Table 4, more electrons transferred during O-terminal adsorption. It was caused by that NO approached substrate with O atom containing greater electronegativity. More electron transferred to NO and weakened N-O bond. Hence, greater change of NO bond length occurred during O-terminal adsorption.

Table 4. The Mulliken charges for N and O atoms in NO molecule.

	N-end	O-end	Free NO
q_N	0.019	-0.023	0.050
q_O	-0.124	-0.181	-0.050
q_{NO}	-0.105	-0.204	0.00

3 conclusions

This research calculated the NO adsorption on clean $CeO_2(110)$ surface or the surface with oxygen vacancy, with periodic slab model by RPBE approach of the generalized

gradient approximation within the framework of density functional theory. The following conclusions are drawn.

(1) NO adsorption was physical with low adsorption energy on clean CeO_2(110) surface. When oxygen vacancy existed on the surface, adsorption significantly increased and chemical adsorption occurred.

(2) The lengthening N-O bond after adsorption was beneficial to further decomposition of NO.

(3) The results under various coverage indicated that the smaller coverage induced more stable adsorption. This was caused by mutual repulsion between NO molecule. Therefore, the adsorption was most stable with the coverage of 0.25mL.

(4)Layout analysis suggested that charges transferred from Ce to NO in the whole system. More charges transferred in O-terminal adsorption than in N-terminal adsorption.

References

[1] J. Kaspar, R. Fomasiero, M. Graziani. *Catal. Today.* **50** (1999)
[2] G. R. Li, D. L. Qu, Z. L. Wang, et al. *Chemistry Common.* **48** (2009)
[3] B. T. Teng, S. Y. Jiang, L. H. Zhao. *J. Chinese Rare Earth Soc.* **28** (2010)
[4] M. Sugiur, M. Ozawa, A. Suda, et al. *Bull. Chem. Soc. Jpn.* **78** (2005)
[5] H. F. Wang. *J. East China univ. sci. technol.* **15** (2012)
[6] G. Li, K. Kaneko, S. Ozeki. *Langmuir.* **1** (1997)
[7] M. Daturi, N. Bion, J. Saussey, et al. *Phys. Chem.* **3** (2001)
[8] M. Gaus, Q. Cui, M. *Elstner. Wires Comput. Mol. Sci.* **4** (2014)
[9] X. Wang, W. K. Chen, X. L. Xu. *Chinese J. Catal.* **28** (2007)
[10] X. Wang, W. K. Chen, B. Z. Su. *Chinese J. Inorg. Chem.* **23 (**2007)
[11] K. Lejaeghere, V. Speybroeck, G. Ost, et al. *Crit. Rev. Solid State Mater. Sci.* **39** (2014)
[12] W. Kohn, A. D. Becke, R. G. Parr. *J. Phys. Chem.* **100** (1996)
[13] G. X. Luo, Z. H. Li, Z. X. Yang. J. Chin. *Rare Earth Soc.* **25** (2007)
[14] R. O. Jones, O. Gunnarsson. *Rev. Mod. Phys.* **61** (1989)
[15] S. Q. Shi, Y. H. Tang, C. Y. Ouyang, et al. *J. Phys. Chem. Solids.* **77** (2010)
[16] M. Nolan, J. E. Fearon, G. W. Watson. *Solid State Ionics.* **777** (2006)
[17] D. O. Scanlon, N. M. Galea, B. J. Morgan, et al. *J. Phys. Chem. C.* **775** (2009)
[18] M. Nolan. *J. Mater. Chem.* **27** (2011)
[19] L. H. Thomas. *Mathematical Proceedings of the Cambridge Philosophical Soc.* **25** (1927)
[20] S. Y. Jiang, B. T. Teng, J. H. Yuan. *Acta Phys. Sin-Ch Ed.* **25** (2009)
[21] N. Michael, G. Sonja, C. Dean. *Surf. Sci.* **57** (2005)
[22] X. T. Thi, C. Stephen, C. Parkerband. *J. Chem. Soc.* **26** (1992)
[23] X. Y. Zong, M. F. Zhao, W. W. Yan. *Chem. Phys. Lett.* **45** (2008)
[24] M. Daturi, N. Bion, J. Saussey, et al. *J. Phys. Chem.* **5** (2001)
[25] G. Herzberg. *New York: Lancaster.*1946.
[26] X. Y Zong，K. Tom, K. Hermansson. *J. Chem. Phys.* **124** (2006)
[27] D. Adam. *J. Phys. Chem. C.* **112** (2008)